Available online at www.sciencedirect.com
ScienceDirect
Ceramics International 35 (2009) 1877–1882
CERAMICS INTERNATIONAL
www.elsevier.com/locate/ceramint

Microstructure and deposition mechanism of CVD amorphous boron carbide coatings deposited on SiC substrates at low temperature

Bin Zeng [a], Zude Feng [a,*], Siwei Li [a], Yongsheng Liu [b], Laifei Cheng [b], Litong Zhang [b]

[a] *Fujian Key Laboratory of Advanced Materials, College of Materials, Xiamen University, Xiamen 361005, China*
[b] *National Key Laboratory of Thermostructure Composite Materials, Northwestern Polytechnical University, Xi'an 710072, China*

Received 7 April 2008; received in revised form 11 September 2008; accepted 18 October 2008
Available online 17 November 2008

Abstract

Amorphous boron carbide (α-B_4C) coatings were prepared on SiC substrates by chemical vapor deposition (CVD) from $CH_4/BCl_3/H_2/Ar$ mixtures at low temperature (900–1050 °C) and reduced pressure (10 kPa). The deposited coatings were characterized using scanning electron microscopy (SEM), X-ray diffraction (XRD), micro-Raman spectroscopy, energy dispersive X-ray spectroscopy (EDS) and X-ray photoelectron spectroscopy (XPS). The results showed that two kinds of α-B_4C coatings were deposited with different microstructures and phase compositions, and the effect of deposition temperature was significant. When deposited at 1000 °C and 1050 °C, the coatings exhibited a nodular morphology and had a relatively low content of boron. The free carbon was distributed in them inhomogeneously; in contrast, when deposited at 900 °C and 950 °C, the coatings presented a comparatively flat morphology and had a uniform internal structure and high boron content. They did not contain free carbon. At the last of this paper, the pertinent mechanisms resulting in differences in microstructure and phase composition were discussed.

Keywords: CVD; Microstructure; Boron carbide coating; Deposition mechanism

1. Introduction

Sequenced self-sealing matrices, which are composed of three layers (SiC layer, α-B_4C layer, Si–B–C layer), have been developed to improve the high temperature durability of $SiC_{(f)}/PyC_{(i)}/[Si,C,B]_{(m)}$ composites [1]. α-B_4C can be infiltrated into the SiC fibrous performs by using $BCl_3/CH_4/H_2$ precursor. Such a CVD system has been widely studied by using cold-wall reactors at relatively high temperature ($T > 1000$ °C) and either at reduced [2–4] or atmospheric pressure [5–7]. Vandenbulcke [6] proposed a mass transfer-equilibrium model and studied the relationship between deposition mechanism and the structure/composition of the deposits. He pointed out that the deposits were badly crystallized or amorphous under conditions of high departure from equilibrium and low temperature. In the work of Jansson's group [2], the thermodynamic calculation was performed for the experimental conditions. The calculation showed that almost all of the CH_4 in the vapor would react to form crystalline B_4C and graphite, and the temperature had only a minor influence on the different heterogeneous equilibria. However, the theoretical prediction was not experimentally confirmed. Therefore, they concluded that the CVD process took place far from equilibrium and the thermodynamic modeling was not sufficient to represent experimental deposition conditions.

The chemical vapor infiltration of a ceramic within fibrous preforms requires a hot-wall reactor operating at low temperature and reduced pressure in order to promote the mass transfer with respect to chemical reaction rates [8], but such conditions for B_4C deposition were not explored in the previous works [9] except for the studies of Hannache et al. [10] and Berjonneau et al. [11]. Hannache et al. mainly studied the kinetics of CVD process of B_4C. Berjonneau et al. prepared α-B_4C coatings in a hot-wall reactor at low temperature (800–1050 °C) and reduced pressure (12 kPa), and explored the relationship between phase composition and deposition condition, but their microstructural characteristics were not reported.

The influence of microstructure on the properties of B_4C is of great interest for engineering application. Most of the

---

* Corresponding author. Tel.: +86 592 2181538; fax: +86 592 2183937.
E-mail address: zdfeng@xmu.edu.cn (Z. Feng).

0272-8842/$34.00 © 2008 Elsevier Ltd and Techna Group S.r.l. All rights reserved.
doi:10.1016/j.ceramint.2008.10.020

investigations on the microstructure and phase composition of CVD B_4C were performed on crystalline material [2,4,7]. According to Olsson et al. [12], the α-B_4C produced at low deposition temperature (1052 °C) showed an extremely complex microstructure through TEM analysis. Vandenbulcke [6] also found that their prepared amorphous boron carbide coatings exhibited a typical nodular morphology. However, there is still lack of a detailed investigation on microstructure and phase composition of α-B_4C coatings.

Karaman et al. [13,14], who used an impinging jet reactor, carried out a systematic kinetic study of B_4C coating deposition from $BCl_3/CH_4/H_2$ and proposed a deposition mechanism. The kinetic analysis showed that the substrate temperature (1000–1400 °C) had a significant effect on the formation rate of B_4C, and the rate of B_4C formation reaction would increase with the increment of CH_4 or BCl_3 mole fraction in the inlet stream. The proposed deposition mechanism indicated that B_4C was produced through a series of surface reactions, which could be described as follows: boron trichloride was adsorbed on the surface non-dissociatively, whereas hydrogen and methane were adsorbed dissociatively. BC was formed on the solid surface through the reaction of adsorbed boron trichloride with adsorbed methane in the form of $CH_3(s)$. Produced BC was reacted in successive series reactions including adsorbed boron trichloride and adsorbed hydrogen to form B_4C.

In this paper, the α-B_4C coatings were deposited on SiC substrates using a hot-wall reactor at low temperature (900–1050 °C) and reduced pressure (10 kPa), and their microstructure and phase composition were investigated. Then the deposition mechanisms of α-B_4C were discussed in the light of the results of microscopic analysis.

2. Experimental

α-B_4C coatings were prepared in a vertical hot-wall reactor (inner diameter, 200 mm) at a total pressure of 10 kPa and in the temperature range of 900–1050 °C. The deposition time was kept at 30 h. The reaction gas mixtures contained BCl_3, CH_4, H_2 and Ar, and the purities of them were all more than 99.99 vol.%.

The total pressure in the reaction vessel was measured using a pressure transducer, and the flow rates of the gases were measured and regulated by mass flow meters. The CH_4 gas flow, the Ar carrier gas flow and the mole fraction of H_2 to BCl_3 in the inlet gas was fixed at 100 cm^3/min, 500 cm^3/min and 2 in all the experiments, respectively. The BCl_3 gas flow varied between 100 cm^3/min and 500 cm^3/min. SiC substrate materials were prepared by depositing 40–50 μm thick 3C–SiC films on graphite slices (30 mm × 15 mm × 2 mm).

The morphology of the coatings was examined by SEM (Leo 1530, Hitachi S-4700 and XL 30 ESEM-TMP). Their phase compositions were investigated by XRD (X'pert PRO) and Raman spectroscopy (Dilor LabRam I). EDS (EDAX) and XPS (PHI Quantum 2000) were used to analyze the relative concentration and chemical bonding states of boron and carbon elements.

Table 1
Deposition parameter, thickness and B/C atomic ratio of the α-B_4C coatings.

δ	T (°C)	Thickness (μm)	Boron/carbon atomic ratio
1	900	0	22.3/77.5
1	950	0	25.4/74.0
1	1000	0	23.7/75.9
1	1050	0	25.5/74.0
3	900	2.7	78.8/20.6
3	950	5.4	64.0/36.0
3	1000	5.4	42.6/53.9
3	1050	5.7	44.9/54.2
5	900	23.8	78.6/21.1
5	950	11.5	78.4/16.7
5	1000	2.6	45.4/53.5
5	1050	4.5	48.3/50.4

3. Results and discussion

The conditions and results of present experiments are summarized in Table 1. The table shows the initial mole ratio of $BCl_3:CH_4$ (δ), deposition temperature (T), thickness and boron/carbon atomic ratio of the coatings. The thickness of the coatings was measured on the cross-sectional SEM micrographs, and each thickness was reported as an average of 10 measurements.

3.1. Microstructure and phase composition

The surface and cross-sectional morphology of all the specimens were observed with SEM. No coating or no continuous coating was observed at the initial mole ratio of $BCl_3:CH_4 = 1$. The coatings deposited at $T = 900$ °C/950 °C, $\delta = 3/5$ showed a comparatively flat morphology and a uniform internal structure (Fig. 1(a) and (b)), however, when deposited at $T = 1000$ °C/1050 °C, $\delta = 3/5$, the coatings showed a micro-scale nodular surface morphology and an inhomogeneous distribution of second phase pyrocarbon (PyC) on the cross-section (Fig. 1(c) and (d)).

The B/C atomic ratio of the coatings and the uncoated specimens were determined from EDS surface scan analysis, which is shown in Table 1. Oxygen made up the balance of the elements in these coatings without considering Si content. It was found that B content was the highest in the coatings deposited at 900 °C/950 °C, second in the coatings deposited at 1000 °C/1050 °C and lowest in the uncoated specimens. The distribution of B and C in the coatings was investigated by EDS point analysis, and the results indicated that it was homogenous for the coatings deposited at 900 °C/950 °C, but there existed second phase PyC distributing inhomogeneously in the coatings deposited at 1000 °C/1050 °C.

XRD analysis showed that no B_4C crystalline phase existed in all coatings, but the low crystallinity PyC was detected in the coatings deposited at $T = 1000$ °C/1050 °C. Fig. 2 shows the XRD patterns of the specimens deposited at $T = 900$ °C, 950 °C, 1000 °C, 1050 °C and $\delta = 5$. The XRD peaks denoted by filled circles and filled rectangles correspond to the peaks of PyC phase and SiC substrates, respectively. The low-intensity diffraction peaks arising from PyC phase indicate its presence

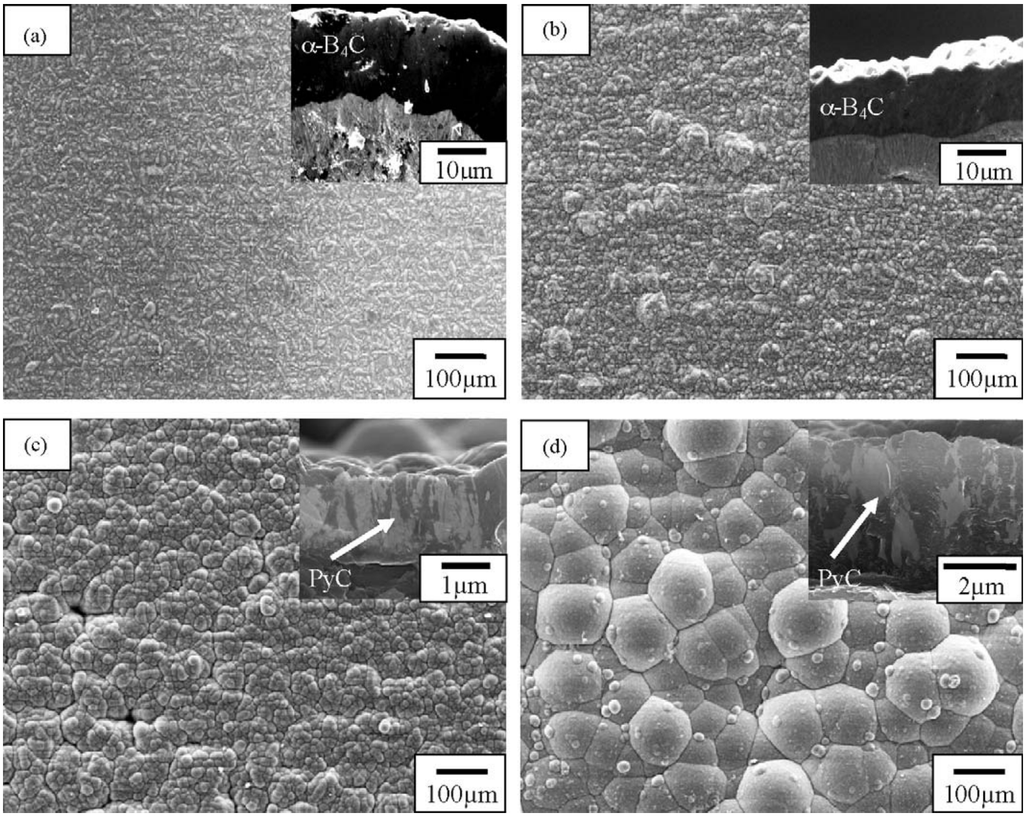

Fig. 1. Surface and cross-section morphology of the α-B_4C coatings deposited at (a) $T = 900\ ^\circ C$, $\delta = 5$; (b) $T = 950\ ^\circ C$, $\delta = 5$; (c) $T = 1000\ ^\circ C$, $\delta = 5$; and (d) $T = 1050\ ^\circ C$, $\delta = 5$.

in the lowly ordered crystalline state in the coatings deposited at $T = 1000\ ^\circ C$, $\delta = 5$ and $1050\ ^\circ C$, $\delta = 5$.

Fig. 3 shows the Raman spectra of eight coated specimens. Two distinct types of Raman spectra of these α-B_4C coatings were observed, suggesting that two kinds of coatings with different microstructure and phase composition were prepared. In Fig. 3, the narrow band at 480 cm^{-1} is associated with the stretching C–B–C chains and the 532 cm^{-1} peak represents the librational mode of $B_{11}C$ icosahedron [15–17]. The multiple Raman bands ranging from 700 cm^{-1} to 900 cm^{-1} have been assigned to the intraicosahedral or intericosahedral B–B bonds [15]. The peak at 980 cm^{-1} is related to the chain rotating and the 1060 cm^{-1} peak corresponds to the breathing modes of the icosahedral $B_{11}C$ structure [15,17,18]. The bands at 1332 cm^{-1} (D-band) and 1580 cm^{-1} (G-band) are attributed to the presence of free carbon in α-B_4C. According to the results in Fig. 3, there was a certain content of free carbon and no B–B bonds in the coatings deposited at 1000 °C and 1050 °C, contrarily, no free carbon could be detected in the coatings deposited at 900 °C and 950 °C.

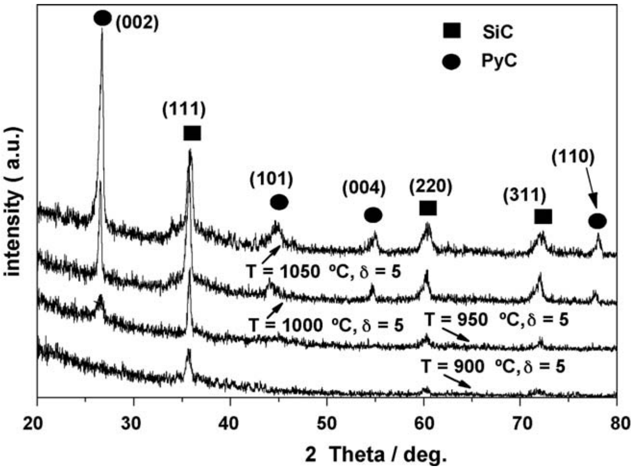

Fig. 2. XRD patterns of the α-B_4C coatings deposited at $T = 900\ ^\circ C$, $950\ ^\circ C$, $1000\ ^\circ C$, $1050\ ^\circ C$ and $\delta = 5$.

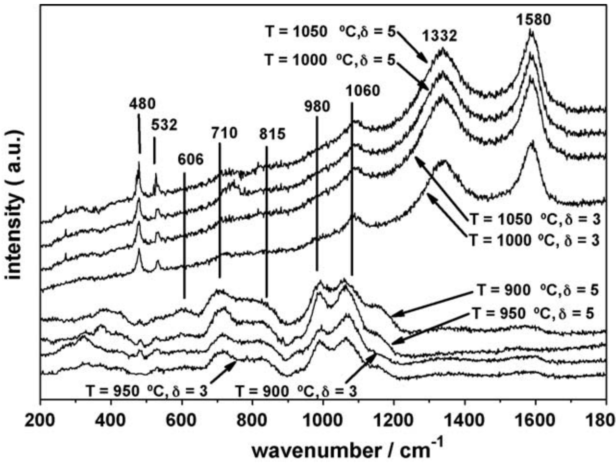

Fig. 3. Raman spectra of α-B_4C coatings at different deposition temperature and initial mole ratio of BCl_3 to CH_4.

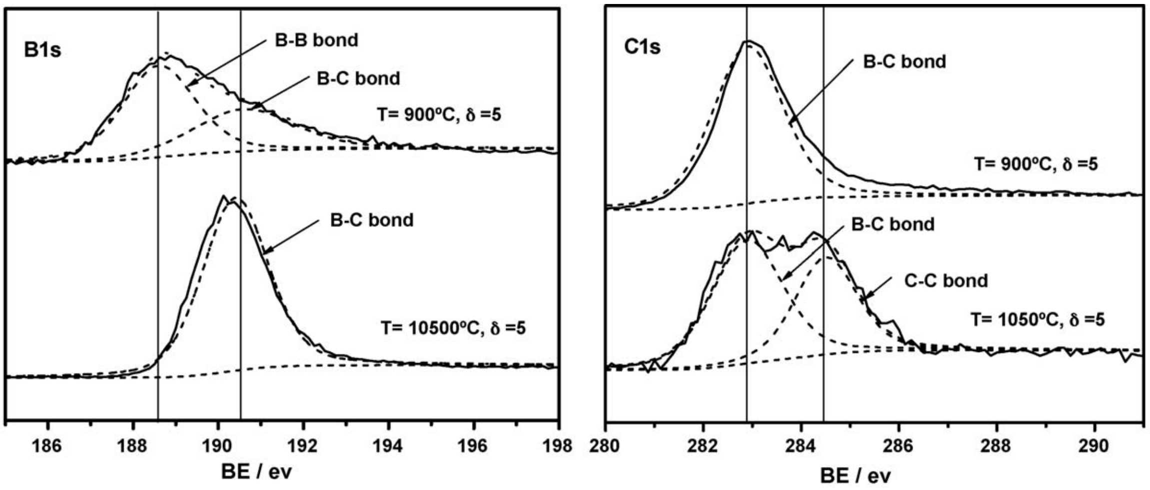

Fig. 4. XPS narrow-scan spectra and the fitted results of B 1s and C 1s of the α-B_4C coatings deposited at $T = 1050$ °C, $\delta = 5$ and $T = 900$ °C, $\delta = 5$.

XPS analysis revealed the presence of boron–carbon compounds in all coatings and the difference of chemical environment of boron and carbon element in the two kinds of α-B_4C coatings. Fig. 4 shows the XPS narrow-scan spectra and the fitted results of B 1s and C 1s from the two coatings deposited at $T = 1050$ °C, $\delta = 5$ and $T = 900$ °C, $\delta = 5$. Both the peak at 190.6 eV in the B 1s spectra and the peak at 282.9 eV in the C 1s spectra indicate the existence of the B–C bonds in the coatings [19], and the peaks at 188.6 eV and 284.4 eV is attributed to B–B bonds in amorphous B_4C [19] and C–C bonds in free carbon phase [20], respectively. The B 1s and C 1s binding energy differences between the two coatings revealed that their phase composition was obviously different.

3.2. Deposition mechanism

As mentioned above, the complete differences in microstructure as well as phase composition were observed between the two kinds of coatings, suggesting that they were deposited through different mechanisms.

When deposited at $T = 1000$ °C/1050 °C, $\delta = 3/5$, the coatings consisted of two phases: α-B_4C phase and PyC phase. This resulted in high content of C in the coatings, suggesting that C-containing growth species played an important role in the deposition process. In order to further explore the deposition mechanism, TEM observations were performed at the coating/matrix interfaces, the result of the specimen deposited at $T = 1050$ °C, $\delta = 5$ is shown in Fig. 5(a). It was found that an interlayer was formed between α-B_4C coating and SiC substrate, and this interlayer was identified as PyC by EDS attached to the TEM. Therefore, it can be deduced that this kind of α-B_4C coatings was formed due to the deposition of carbon atoms and the presence of PyC, and the result also implied that the deposition of carbon induced the subsequent deposition of boron atoms. This may be attributed to the decrease in surface free energy of sorption for the B-containing growth species, which made the absorption of B-containing growth species at the solid surface much easier than that on the SiC substrate. On the other hand, no B–B bond was found by Raman and XPS analysis, indicating that no boron clusters were formed in the CVD process. This result further

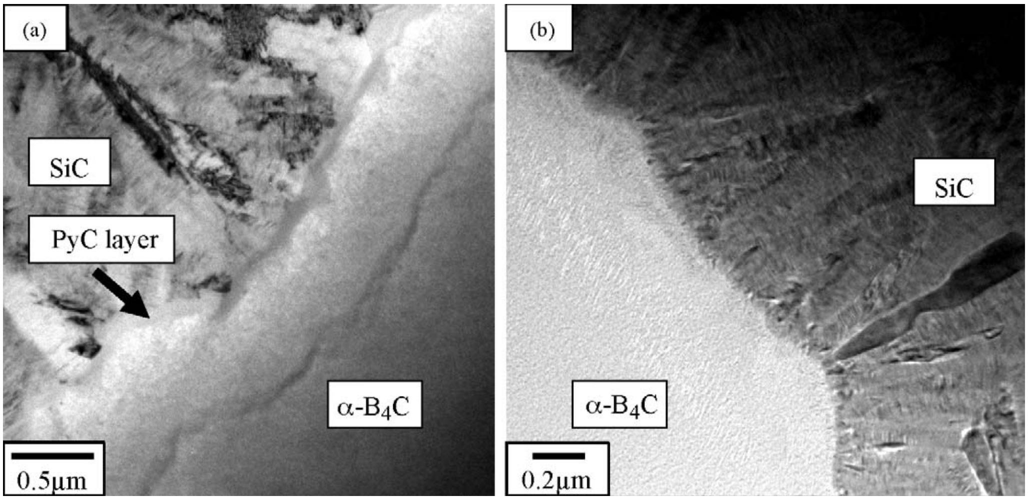

Fig. 5. TEM micrographs of the coating/matrix interfaces of the α-B_4C coatings deposited at (a) $T = 1050$ °C, $\delta = 5$ and (b) $T = 900$ °C, $\delta = 5$.

suggested that the B-containing growth species likely adsorbed dispersedly and then reacted with C-containing growth species abundantly existing on solid surface to form solid deposit α-B_4C, so the deposition of carbon, to a great extent, would affect the microstructure and phase composition of these coatings. Based on the above discussion, this kind of α-B_4C coatings can be formed in terms of following steps: (1) the C-containing growth species were adsorbed on SiC substrate to form PyC interlayer; (2) B-containing growth species was then adsorbed onto PyC and reacted with adsorbed C-containing growth species to produce B–C compounds, which was followed by the formation of B–C nodule (Fig. 1(c) and (d)); (3) nodules coalesced to form a B–C solid layer.

When deposited at $T = 900$ °C/950 °C, $\delta = 3/5$, the coatings did not contain free carbon, but had a high content of boron, which suggested that the B-containing growth species would play an important role in the formation of these coatings during the deposition process. TEM was also used to examine the interface structure. It was found that there existed no interlayer between coating and SiC substrate (see Fig. 5(b)). This result showed that the mechanism of this kind of α-B_4C coating was obviously different from that previously mentioned, and the coatings could be produced without preferential deposition of PyC from C-containing growth species. Therefore, at the beginning of deposition, the B–C compounds were probably formed directly from B-containing growth species and C-containing growth species, which both were adsorbed on SiC substrates. In addition, both Raman and XPS analysis showed the presence of B–B bonds in the deposited coatings, apparently boron clusters were generated during the deposition process, suggesting that a great amount of B-containing growth species could be adsorbed and deposited onto solid surface. By comparing the Raman spectra, it was found that the spectra of the deposited coatings are similar to that of crystalline B_4C [21], however, the intensity of the bands in the low-frequency region (<600 cm^{-1}) of the former was much weaker than the latter. Both the difference and similarity revealed that the coatings had poor crystallinity and tended to transform into crystalline ones. According to Karaman et al. [13], who prepared the crystalline B_4C coatings by CVD technique, C-containing growth species were only involved in the formation of the intermediate products of B_4C, while B-containing growth species participated in the whole process of B_4C molecules formation. This implied that B-containing growth species determined the final formation of B_4C molecules. Based on the factors mentioned above, we concluded that B-containing growth species played a critical role in the formation of these coatings, and the coating deposition originated from direct nucleation between B-containing growth species and C-containing growth species, so this kind of α-B_4C coatings can be formed according to the following steps: (1) B-containing growth species and C-containing growth species were adsorbed onto solid surface and then reacted to produce B–C compounds; and (2) the B–C compounds were deposited continuously to produce a B–C solid layer.

Thermodynamic analysis of the B–C–H–Cl had shown that $HBCl_2$ was an intermediate and/or byproduct [22], which was formed by hydrogen reduction of BCl_3, this conclusion was also confirmed by experiments in the work of several researchers [6,9,11,14]. When $\delta = 1$, the concentrations of BCl_3 was very low, so the supersaturation conditions for B_4C deposition could not be achieved, the coating could not be deposited. On the other hand, the low initial concentration of BCl_3 could reduce hydrogen consumption, and then a high concentration of hydrogen was maintained in the mixed gases, which prevented the pyrogenation process of CH_4 and resulted in no observable coating, furthermore, the methane molecules (more or less fragmented) could be strongly adsorbed on the substrate, which would reduce the adsorption as well as the surface diffusion of the boron-carrying species [3], and would inhibit deposit formation.

Thermodynamic method was used to estimate the temperature threshold (T_t) for carbon-rich α-B_4C deposition. The equation of the formation reaction of carbon-rich α-B_4C could be expressed this way:

$$8BCl_3(g) + 5CH_4(g) + 2H_2(g) \rightarrow 2\alpha\text{-}B_4C(g) + 3C(s) + 24HCl(g)$$

If this reaction could occur spontaneously, then the standard free energy change must be negative:

$$\Delta G^{\theta} = \Delta H^{\theta} - T\Delta S^{\theta} \le 0$$

where ΔG^{θ} is the standard change in Gibbs energy (kJ mol^{-1}), ΔH^{θ} denotes the standard change of the reaction enthalpy (kJ mol^{-1}), ΔS^{θ} is the standard change of the reaction entropy (J mol^{-1} K^{-1}), and T is the temperature (K). The thermodynamics data (see Table 2) were taken from the NIST Chemistry WebBook [23] (because the thermodynamic data of substoichiometric boron carbides was in shortage and the standard molar entropy and standard molar enthalpy of B_4C did not affect the calculation results greatly, we used the themodynamics data of crystal B_4C to calculate T_t). Ignoring the effect of temperature on ΔH^{θ} and ΔS^{θ}, T_t was evaluated:

$$T_t \ge \frac{\Delta H^{\theta}}{\Delta S^{\theta}} = \frac{1257.37\,\text{kJ mol}^{-1}}{1029.72\,\text{kJ mol}^{-1}} = 1221\,\text{K} = 948\,^{\circ}\text{C}$$

The calculated result indicated that carbon-rich α-B_4C coatings could be deposited at the temperature more than 948 °C, which was in good agreement with the experiment results and the above mechanism analysis.

Table 2
Standard enthalpy of formation and standard entropy values of reactants and products for carbon-rich α-B_4C deposition reaction.

Material	$\Delta_f H_m^{\theta}$ (kJ mol^{-1})	ΔS_m^{θ} (J mol^{-1} K^{-1})
$B_4C(s)$	−62.68	26.72
$CH_4(g)$	−74.85	188.68
$H_2(g)$	0	130.68
$BCl_3(g)$	−402.96	290.17
HCl(g)	−92.3	186.9
$C_{graphite}$	0	5.6

4. Conclusion

The α-B_4C coatings were deposited on SiC substrates in a hot-wall reactor from $BCl_3/CH_4/H_2/Ar$ mixtures at low temperature (900–1050 °C) and reduced pressure (10 kPa). Two kinds of α-B_4C coatings with different microstructures and phase compositions were found, and the deposition temperature was an important influencing factor. At 1000 °C and 1050 °C, the coatings formation was due to the nucleation of C atoms and the deposition of PyC interlayer. C-containing growth species played a very important role in the deposition process. The coatings exhibited a nodular morphology and had a relatively low content of boron. The free carbon distributed in it inhomogeneously; in contrast, at 900 °C and 950 °C, the coatings were deposited directly from B-containing growth species and C-containing growth species on SiC substrates without the induction of PyC nucleation layer. The B-containing growth species had a crucial effect on coating deposition. They presented a comparatively flat morphology and had a uniform internal structure and high boron content. No free carbon was produced in them.

Acknowledgments

This work was financially supported by National Natural Science Foundation of China (Nos. 50532010 and 90405015) and the Doctorate Foundation of Northwestern Polytechnical University (CX200505).

Reference

[1] L. Quemard, F. Rebillat, A. Guette, H. Tawil, C. Louchet-Pouillerie, Self-healing mechanisms of a SiC fiber reinforced multi-layered ceramic matrix composite in high pressure steam environments, J. Eur. Ceram. Soc. 27 (2007) 2085–2094.

[2] U. Jansson, J.O. Carlsson, B. Stridh, S. Soderberg, M. Olson, Chemical vapor deposition of boron carbides I: phase and chemical composition, Thin Solid Films 172 (1989) 81–93.

[3] U. Jasson, J.O. Carlsson, Chemical vapor deposition of boron carbides in the temperature range 1300–1500 K and at a reduced pressure, Thin Solid Films 124 (1985) 101–107.

[4] T.S. Moss, W.J. Lackey, K.L. More, Chemical vapor deposition of $B_{13}C_2$ from BCl_3–CH_4–H_2–argon mixtures, J. Am. Chem. Soc. 81 (1998) 3077–3086.

[5] L. Vandenbulcke, R. Herbin, M. Basutcu, J.N. Barrandon, Étude expérimentale du dépôt chimique du carbure de bore àpartir de mélanges trichlorure de bore, méthane et hydrogène, J. Less-Common Metals 80 (1981) 7–22.

[6] L. Vandenbulcke, Theoretical and experimental studies on the chemical vapor deposition of boron carbide, Ind. Eng. Chem. Process Des. Dev. 24 (1985) 568–575.

[7] S.N. Dilek, H.O. Ozbelge, N.A. Sezgi, T. Dogu, Kinetic studies for boron carbide formation in a dual impinging-jet reactor, Ind. Eng. Chem. Res. 40 (2001) 751–755.

[8] F. Langlais, Chemical vapor infiltration processing of ceramic matrix composites, in: A. Kelly, C. Zweben (Eds.), Comprehensive Composite Materials, Pergamon Press, Oxford, 2000, pp. 611–644.

[9] J. Berjonneau, F. Langlais, G. Chollon, Understanding the CVD process of (Si)–B–C ceramics through FTIR spectroscopy gas phase analysis, Surf. Coat. Technol. 201 (2007) 7273–7285.

[10] H. Hannache, F. Langlais, R. Naslain, Kinetics of boron carbide chemical vapor deposition and infiltration, in: J.O. Carlsson, J. Lindström (Eds.), Proceedings of the 5th European Conference on CVD, Uppsala, Sweden, (1985), pp. 219–233.

[11] J. Berjonneau, G. Chollon, F. Langlais, Deposition process of amorphous boron carbide from $CH_4/BCl_3/H_2$ precursor, J. Electrochem. Soc. 153 (2006) C795–C800.

[12] M. Olsson, U. Jansson, B. Stridh, S. Soederberg, J.O. Carlsson, Mechanical and tribological properties of chemical vapour deposition boron carbide coatings, Proceedings of the 3rd International Conference on the Science of Hard Materials, Nassau, Bahamas, 1987, in Mater. Sci. Eng. A 105–106 (1988) 453–463.

[13] M. Karaman, H.Ö. Özbelge, N.A. Sezgi, T. Dogu, Mechanism and characterization studies on boron carbides deposited by chemical vapor deposition technique, Mater. Res. Soc. Symp. Proc. 886 (2006), 0886-F11-11.1.

[14] M. Karaman, N.A. Sezgi, T. Dogu, H.Ö. Özbelge, Kinetic investigation of chemical vapor deposition of B_4C on tungsten substrate, AIChE J. 52 (2006) 4161–4166.

[15] X.Q. Yan, W.J. Li, T. Goto, M.W. Chen, Raman spectroscopy of pressure-induced amorphous boron carbide, Appl. Phys. Lett. 88 (2006), 131905-1–131905-3.

[16] R. Lazzari, N. Vast, J.M. Besson, S. Baroni, A.D. Corso, Structure and vibrational properties of icosahedral B_4C boron carbide, Phys. Rev. Lett. 83 (1999) 3230–3233.

[17] N. Vast, S. Baroni, G. Zerah, J.M. Besson, A. Polian, J.C. Chervin, T. Grimsditch, Lattice dynamics of icosahedral α-boron under pressure, Phys. Rev. Lett. 78 (1997) 693–696.

[18] H. Werheit, H.W. Rotter, F.D. Meyer, H. Hillebrecht, S.O. Shalamberidze, T.G. Abzianidze, G.G. Esadze, FT-Raman spectra of isotope-enriched boron carbide, J. Solid State Chem. 177 (2004) 569–574.

[19] F. Kokai, M. Taniwaki, M. Ishihara, Y. Koga, Effect of laser fluence on the deposition and hardness of boron carbide thin films, Appl. Phys. A 74 (2002) 533–536.

[20] M. R'Mili, V. Massardier, P. Merle, H. Vincent, C. Vincent, The effect of thermal exposure on the strength distribution of B_4C coated carbon fibers, Carbon 37 (1999) 129–145.

[21] N. Vast, J.M. Besson, S. Baroni, A.D. Corso, Atomic structure and vibrational properties of icosahedral α-boron and B_4C boron carbide, Comput. Mater. Sci. 17 (2000) 127–132.

[22] M. Ducarroir, C. Bernard, Thermodynamic domains of the various solid deposits in the B–C–H–CI vapor system, J. Electrochem. Soc. 123 (1976) 136–140.

[23] The NIST Chemistry WebBook, http://webbook.nist.gov/chemistry/.